# Three-nucleon force effects in nucleon induced deuteron breakup. II. Comparison to data

J. Kuroś-Żołnierczuk,[1] H. Witała,[1] J. Golak,[1,2] H. Kamada,[3] A. Nogga,[4] R. Skibiński,[1] and W. Glöckle[2]
[1]*M. Smoluchowski Institute of Physics, Jagiellonian University, Reymonta 4, 30-059 Kraków, Poland*
[2]*Institut für Theoretische Physik II, Ruhr Universität Bochum, D-44780 Bochum, Germany*
[3]*Department of Physics, Faculty of Engineering, Kyushu Institute of Technology, 1-1 Sensucho, Tobata, Kitakyushu 804-8550, Japan*
[4]*Department of Physics, University of Arizona, Tucson, Arizona 85721*
(Received 21 March 2002; published 21 August 2002)

Selected *Nd* breakup data over a wide energy range are compared to solutions of Faddeev equations based on modern high precision *NN* interactions alone and adding current three-nucleon force models. Unfortunately currently available data probe phase space regions for the final three nucleon momenta which are rather insensitive to three-nucleon force (3NF) effects as predicted by current models. Overall there is good to fair agreement between present day theory and experiment but also some cases exist with striking discrepancies. Regions in the phase space are suggested where large 3NF effects can be expected.

DOI: 10.1103/PhysRevC.66.024004 PACS number(s): 21.30.−x, 21.45.+v, 25.10.+s, 24.70.+s

## I. INTRODUCTION

In a previous paper [1], called paper I in the following, we performed a systematic search for three-nucleon force (3NF) effects in the full phase space of the *Nd* breakup process. To that aim we determined the predictions for the fivefold differential breakup cross section and several analyzing powers based on the current high-precision *NN* potentials AV18 [2], CD Bonn [3], Nijm I, II, and Nijm 93 [4] alone. These predictions form a band for each of the observables as a function of the five variables needed for a kinematically complete determination of the breakup process. These five variables define a point in the phase space. Then we added to each of the five *NN* potentials the Tucson-Melbourne (TM) three-nucleon force [5,6] which, with the help of a strong form factor parameter, has been adjusted to the $^3$H binding energy separately for each *NN* force [7]. The predictions for the observables based on these force combinations form another band. We talk of 3NF effects if the two bands are significantly separated. In addition we regarded two special cases, the *NN* and 3NF combinations AV18 + Urbana IX [8] and CD Bonn+TM′, where TM′ is a modified TM 3NF, which corrects a violation of chiral symmetry in TM [9,10]. All the studies have been carried through with fully converged solutions of the Faddeev equations for four nucleon laboratory energies 13, 65, 135, and 200 MeV. In this manner we covered a wide range of energies and could identify the different phase space regions, where for each of the observables 3NF effects, based on the current models, can be expected. It is now the aim of this paper to compare our predictions with existing data. Unfortunately, in contrast to *Nd* elastic scattering, where precise data are numerous (see references in paper I), the existing data base for the breakup process is much less numerous, especially at higher energies. Unfortunately, as we shall see, the phase space regions, where the current models predict large 3NF effects, have not yet been explored experimentally.

Here we cannot display all the existing data. For references to older data (before 1980) we refer to Ref. [11]. We also have to omit a very interesting full phase space search [12]. Unfortunately the access to the data is no longer possible and the documentation in Ref. [12] is insufficient to analyze the data newly. At that time they were analyzed based on pioneering calculations by Kloet and Tjon [13]. They used very simple spin dependent *S*-wave forces, which are highly insufficient by present day standards. Moreover those data had a high statistical error. Therefore we are looking forward to the data currently being taken at KVI Groningen [14–16], which will cover a large part of the phase space, too, and will be much more accurate.

In Sec. II we present a comparison of our theoretical predictions with a selection of more recent breakup data (after 1980). Most of them have been analyzed before by us [11] choosing either older *NN* potentials (Bonn B, AV14, Paris) or only one of the modern ones. Also the addition of 3NFs has not been performed before to such an extent as in this paper. The criteria for the selection of data are, that no averaging according to acceptances and angular openings have to be performed, well documented data are available and the experimental errors are small.[1] Further we favored cases where the same observables were measured by different groups and we tried to cover the total phase space as much as possible. For other data known to us (after 1980) and not shown we provide at least references. We close with a brief summary in Sec. III.

## II. COMPARISON TO THE DATA

There are obviously continuously varying breakup configurations and the experimental groups had to make a choice. Up to now so called specific configurations such as FSI, QFS, STAR, and COLL have mostly been measured. Their meaning will be explained below together with the discussion of the data. We have chosen data at 13 MeV representing the low-energy region and at 65 MeV for the higher-energy region. Recently new data appeared at 200 MeV [17], which we will also show.

As described in the Introduction our theoretical predic-

[1]Because of lack of other data we had to include some with large error bars.

 

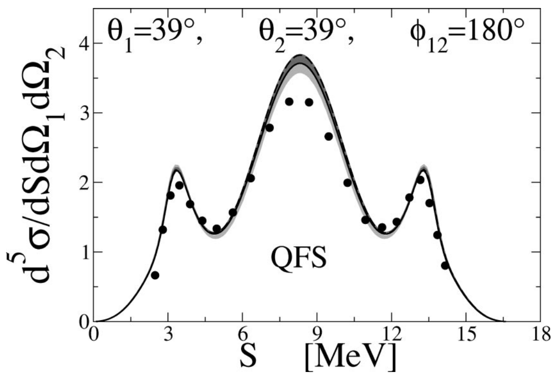


FIG. 1. *Nd* breakup cross section data in mb MeV$^{-1}$sr$^{-2}$ at 13 MeV in comparison to *NN* force predictions alone (light shaded band) and adding the TM 3NF (dark shaded band); further shown is CD Bonn+TM′ (dashed line) and AV18+Urbana IX (solid line). The *pd* data (full circles) are from Ref. [28].

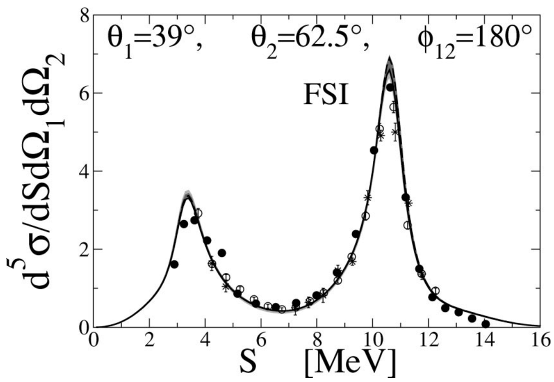


FIG. 2. Nd breakup cross section data in mb MeV$^{-1}$sr$^{-2}$ at 13 MeV in comparison to theoretical predictions. Bands and curves as in Fig. 1. The *nd* data are from Refs. [21] (stars), [18] (open circles), and the *pd* data from Ref. [28] (full circles).

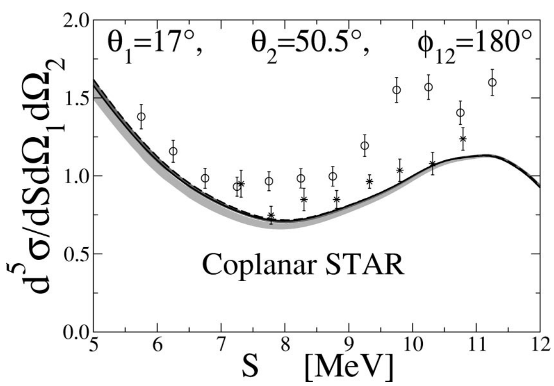


FIG. 3. Nd breakup cross section data in mb MeV$^{-1}$sr$^{-2}$ at 13 MeV in comparison to theoretical predictions. Bands and curves as in Fig. 1. The *nd* data are from Refs. [21] (stars) and [18] (open circles).

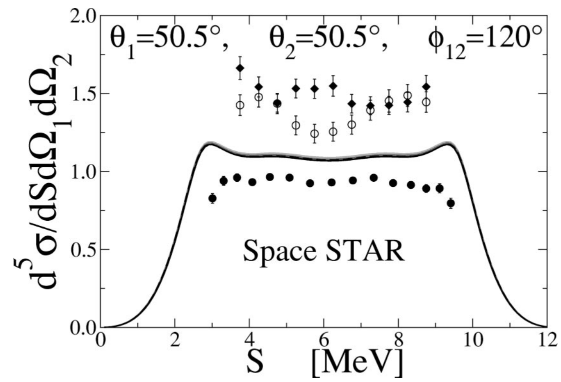


FIG. 4. *Nd* breakup cross section data in mb MeV$^{-1}$sr$^{-2}$ at 13 MeV in comparison to theoretical predictions. Bands and curves as in Fig. 1. The *nd* data are from Refs. [18] (open circles), [23] (full diamonds), and the *pd* data from Ref. [28] (full circles).

tions will be displayed in form of two bands corresponding to *NN* forces only and adding the TM 3NF. In addition there will be two curves for the combinations AV18+Urbana IX and CD Bonn+TM′.

### A. Energy 13 MeV

The majority of the breakup experiments were performed in the region of low energies ($\lesssim 25$ MeV) for both the *nd* [18–26] and the *pd* [27–36] breakup. We compare some of the 13 MeV data with our theoretical predictions for the cross section and nucleon analyzing power $A_y$ in Figs. 1 and 12.

Let us first regard the cross sections which are given at the following special configurations: the quasifree scattering (QFS) geometry, where one of the nucleons in the final state is at rest in the laboratory frame; the final state interaction (FSI) geometry, where the relative energy of two outgoing nucleons is equal to zero; the coplanar STAR geometry, where the three nucleons emerge from the reaction in the c.m. system with coplanar and equal momenta at 120° relative to each other and where the beam lies in that plane and also the symmetric space STAR (SSS) geometry, where the c.m. plane containing the nucleon momenta is perpendicular

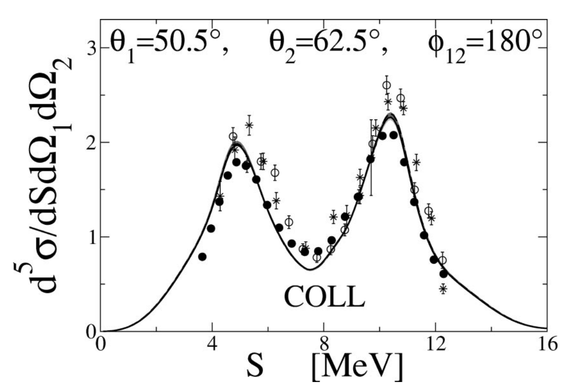


FIG. 5. *Nd* breakup cross section data in mb MeV$^{-1}$sr$^{-2}$ at 13 MeV in comparison to theoretical predictions. Bands and curves as in Fig. 1. The *nd* data are from Refs. [18] (open circles), [18] (open circles), and the *pd* data from Ref. [28] (full circles).

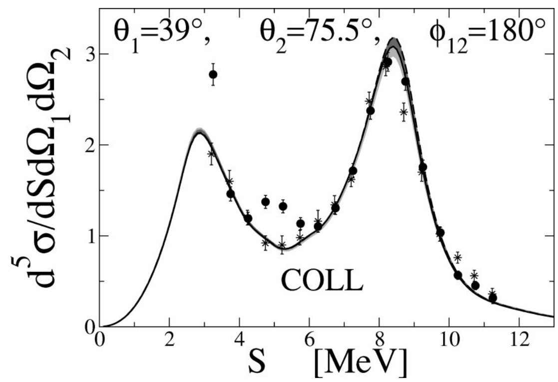


FIG. 6. $Nd$ breakup cross section data in mb MeV$^{-1}$sr$^{-2}$ at 13 MeV in comparison to theoretical predictions. Bands and curves as in Fig. 1. The $nd$ data are from Ref. [21] (stars) and the $pd$ data from Ref. [28] (full circles).

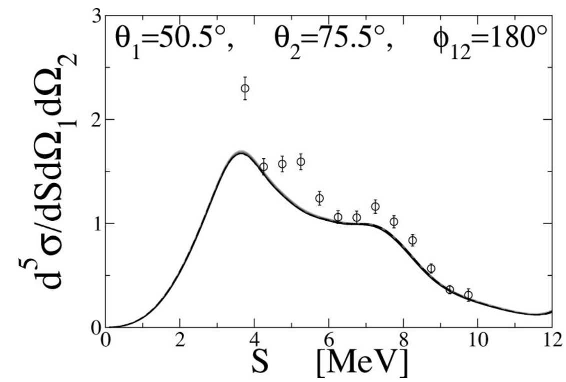


FIG. 7. $Nd$ breakup cross section data in mb MeV$^{-1}$sr$^{-2}$ at 13 MeV in comparison to theoretical predictions. Bands and curves as in Fig. 1. The $nd$ data are from Ref. [18].

to the beam direction; the collinear (COLL) configuration, where one of the nucleons is at rest in the c.m. system and therefore the other two have momenta back to back. In addition two unspecific configurations have been chosen in Figs. 7 and 8.

As is seen in Figs. 1–8 the two bands are only slightly shifted to each other and therefore 3NF effects are very small at this energy. The pure $2N$ force predictions agree in many cases with the data.

Especially interesting is the SSS configuration for which $pd$ [28] as well as $nd$ data taken by different groups [18,21,23] exist. For this configuration our theoretical $nd$ predictions shown in Fig. 4 underestimate the $nd$ data by about 20% and overestimate the $pd$ data by about 15%. The discrepancy for the $pd$ data could probably have its origin in the neglected $pp$ Coulomb force. The origin of the difference to the $nd$ data, called the *space star anomaly* [23], is still unknown. The disagreement here is quite surprising, since the calculations [22] show that the $NN$ $S$-wave contributions are the dominant part in the space star geometry[2] and their properties are rather well determined in the $NN$ system.

The example with an FSI interaction peak shown in Fig. 2 is also very interesting. This type of peak can be used to extract $np$ or $nn$ scattering lengths ($a_{np}$ or $a_{nn}$) in the state $^1S_0$. In such a manner the well known $a_{np}$ could be extracted with the correct value using only $NN$ forces [25,26,37]. In case of $a_{nn}$ there exists a challenging controversy, where two independent $nd$ breakup measurements lead to quite different results [25,37]. One [37] agrees with the usually quoted value found in the $\pi^- d$ absorption process, while the other one [25] is significantly smaller in magnitude.

We also display a coplanar STAR result, where a renewed measurement [21] agrees quite well with present day nuclear force predictions now, while an older one [18] is far off. A corresponding shift of data occurred also for the COLL configuration $(\theta_1,\theta_2,\phi_{12})\equiv(39°,75.5°,180°)$, where the new

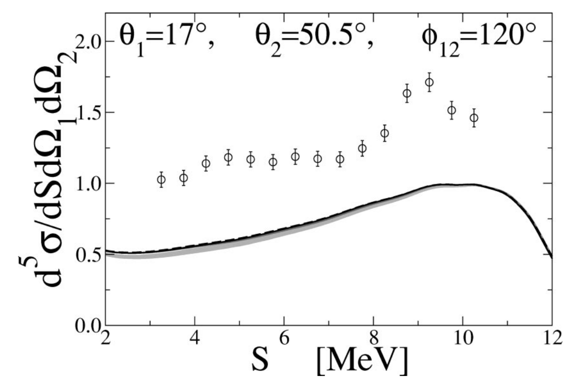


FIG. 8. $Nd$ breakup cross section data in mb MeV$^{-1}$sr$^{-2}$ at 13 MeV in comparison to theoretical predictions. Bands and curves as in Fig. 1. The $nd$ data are from Ref. [18].

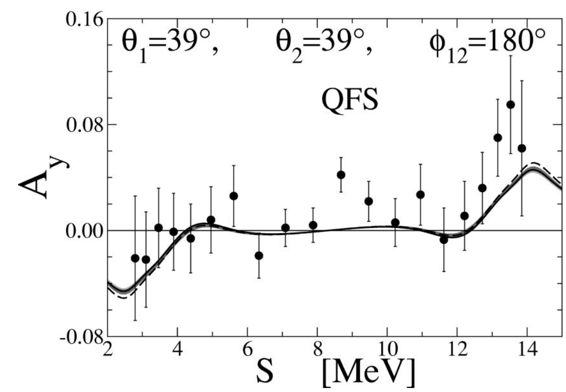


FIG. 9. Nucleon analyzing power $A_y$ data in $Nd$ breakup at 13 MeV in comparison to theory. Bands and curves as in Fig. 1. The $pd$ data are from Ref. [28].

[2]60% of the space star cross section is due to the $^3S_1$ $NN$ force, 30% due to the $^1S_0$ force, and only about 10% comes from the $P$-wave forces [22].

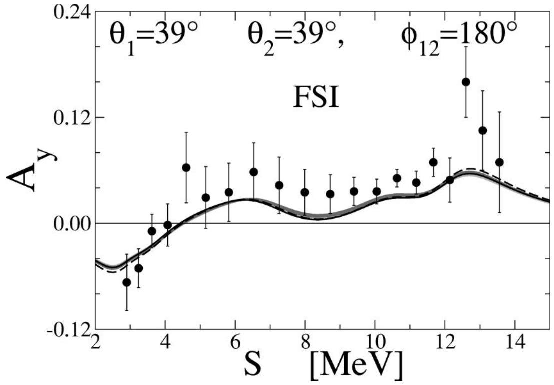


FIG. 10. Nucleon analyzing power $A_y$ data in $Nd$ breakup at 13 MeV in comparison to theory. Bands and curves as in Fig. 1. The $pd$ data are from Ref. [28].

data [21] agree with theory in contrast to the old one [18].

But there are also discrepancies. One example of QFS condition is shown in Fig. 1. It is unknown, whether $pp$ Coulomb force corrections are responsible for those deviation. A more recent measurement [38] also shows the discrepancy for QFS conditions. Very remarkable is also that in one of the two unspecific configurations (17°, 50.5°, 120°) we see a dramatic disagreement of theory and data. A remeasurement would be highly welcome.

For the nucleon analyzing power $A_y$, the agreement to $NN$ force predictions alone is, in general, good (see Figs. 9–12), though, the data scatter and have large error bars. All 3NFs give small effects for this observable in the chosen configurations at this energy.

Further data in the low-energy region can be found in Ref. [11]. The agreement with theory is similar as for the selected examples shown, with some further exceptions in the data set from Erlangen [18,20] and [36].

Now, regarding the information gained in paper I, one has to ask whether the available data probed the phase space regions, where current 3NF models predict significant effects. The answer is unfortunately no. For the breakup cross section the sensitive regions to see 3NF effects at 13 MeV are around $\theta_1=\theta_2=50°$ and $\phi_{12}=170°$. Data there would be very useful. For the analyzing power $A_y$ corresponding

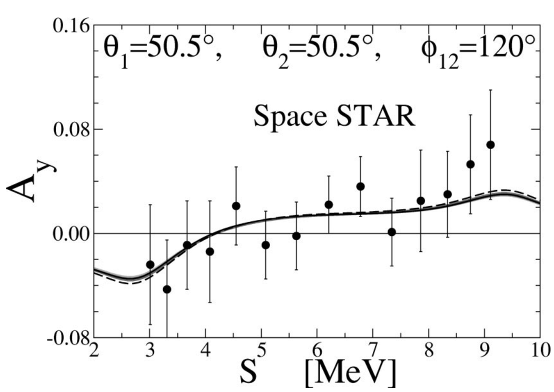


FIG. 11. Nucleon analyzing power $A_y$ data in $Nd$ breakup at 13 MeV in comparison to theory. Bands and curves as in Fig. 1. The $pd$ data are from Ref. [28].

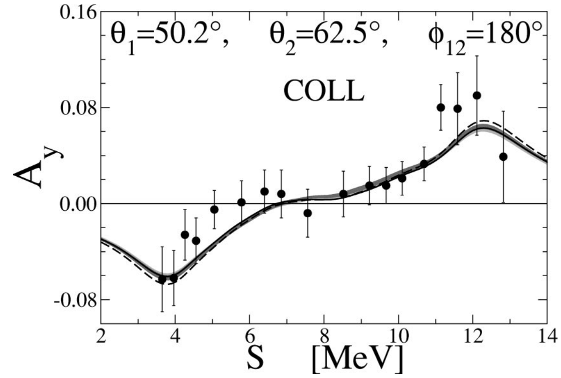


FIG. 12. Nucleon analyzing power $A_y$ data in $Nd$ breakup at 13 MeV in comparison to theory. Bands and curves as in Fig. 1. The $pd$ data are from Ref. [28].

sensitive regions are around $\theta_1=100°$, $\theta_2=30°$ (and vice versa), and $\phi_{12}=160°$. Unfortunately in this case the proton energies are rather small ($\leqslant 3$ MeV).

### B. Energy 65 MeV

At this energy the fivefold differential cross section and the proton analyzing power were measured for the $\vec{d}(p,pp)n$ reaction in 13 different kinematically complete configurations [39–41]. In Figs. 13–25 those data are compared to our theoretical predictions.

Let us first regard the cross sections. In cases where the two bands are narrow and either overlap or are close together

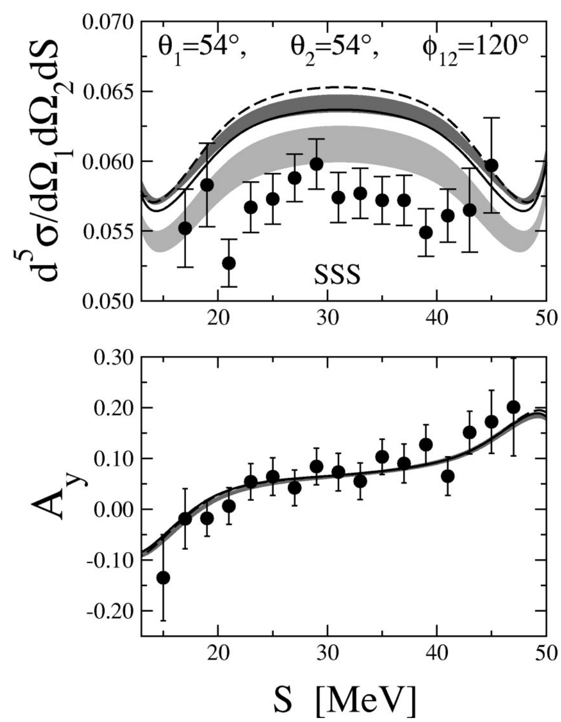


FIG. 13. $Nd$ breakup cross section in mb MeV$^{-1}$sr$^{-2}$ and nucleon analyzing power data at 65 MeV in comparison to theory. Symmetric space star (SSS) configuration is shown. Bands and curves as in Fig. 1. The $pd$ data are from Ref. [40].

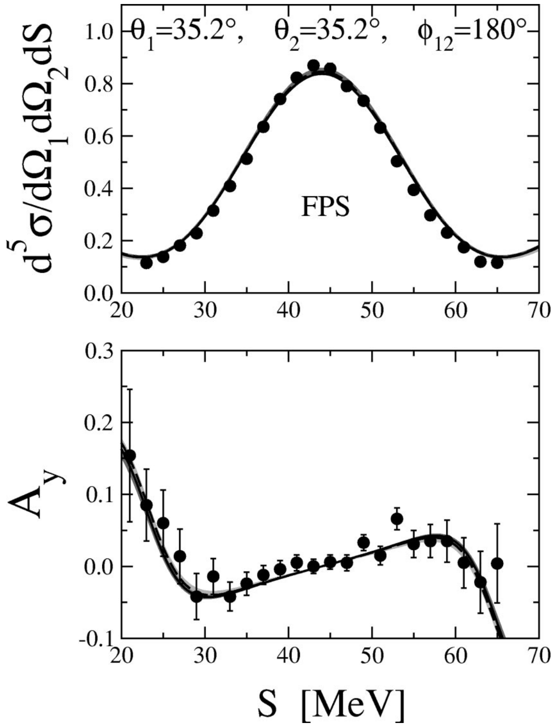


FIG. 14. *Nd* breakup cross section in mb MeV$^{-1}$sr$^{-2}$ and nucleon analyzing power data at 65 MeV in comparison to theory. Symmetric forward star (FPS) configuration is shown. Bands and curves as in Fig. 1. The *pd* data are from Ref. [40].

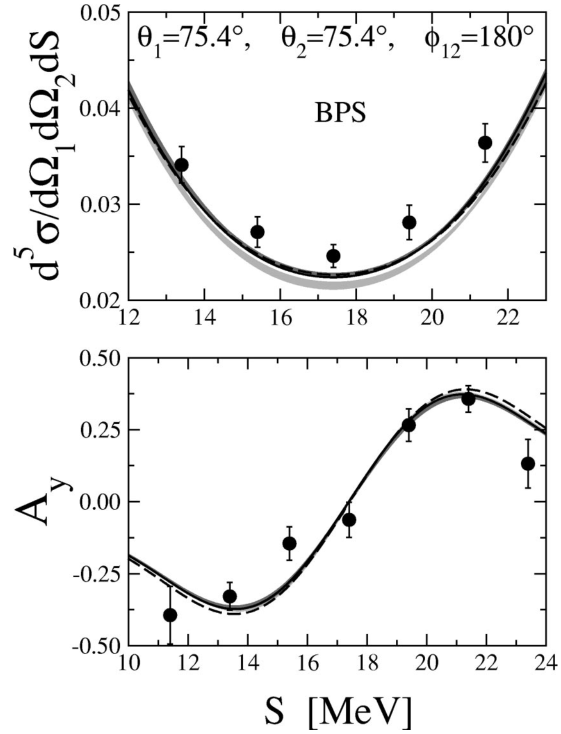


FIG. 15. *Nd* breakup cross section in mb MeV$^{-1}$sr$^{-2}$ and nucleon analyzing power data at 65 MeV in comparison to theory. Backward plane star (BPS) configuration is shown. Bands and curves as in Fig. 1. The *pd* data are from Ref. [40].

the agreement with the data is rather good, with the exception of the two QFS configurations (see Figs. 16,17), a backward plane star (BPS) configuration (see Fig. 15), and an unspecific one (20°, 116.2°, 0°) (see Fig. 25). The BPS configuration denotes the situation where one of the three nucleons goes antiparallel to the beam direction. There is also forward plane star (FPS) configuration where one of the nucleons goes along the beam direction. Note in all cases one should keep in mind that the magnitude of the *pp* Coulomb force effects under the different conditions are not known. For the QFS configurations one might indeed expect small 3NF effects, as we see, since by definition of that configuration one final nucleon is at rest and thus in a simple picture is similar to a spectator to a two-nucleon process. This is, however, not quite right, since that ‘‘spectator nucleon’’ is heavily rescattered as a comparison of the full solution with a plane wave assumption for that nucleon reveals [11,42]. Our results show that, 3NF effects remain thereby small. As we have seen at 13 MeV and what we found at other energies below about 25 MeV, theory overshoots the experimental QFS maxima by about 20%. This decreases but remains still significant at 65 MeV with about 13%. Also the QFS peak at 65 MeV is narrower than the theory predicts. All that might suggest again Coulomb force effects to be mostly responsible for the discrepancies. There are indeed first steps (based on low rank *NN* forces) which point to quite large Coulomb force effects for the breakup cross section [43].

In the two cases in Fig. 13 and 19 where the two bands are distinct (say larger than 10%) the situation is controversial. In one case (SSS) *NN* predictions alone touch at least

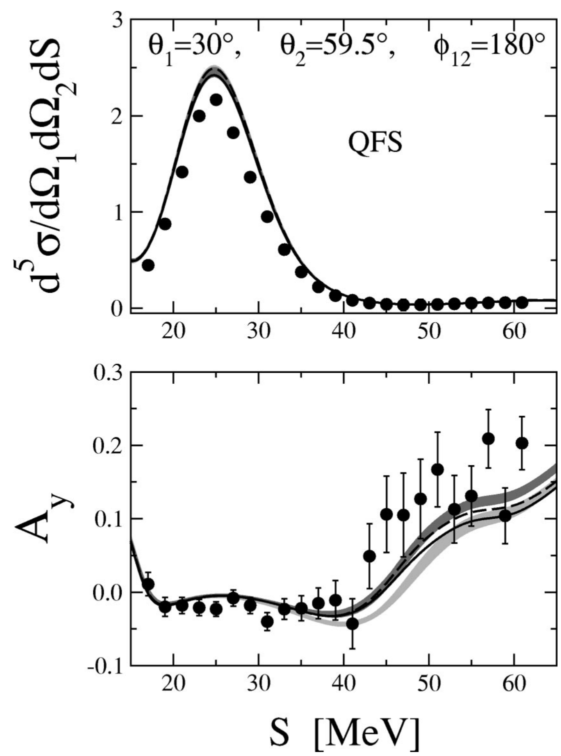


FIG. 16. *Nd* breakup cross section in mb MeV$^{-1}$sr$^{-2}$ and nucleon analyzing power data at 65 MeV in comparison to theory. Quasifree scattering (QFS) configuration is shown. Bands and curves as in Fig. 1. The *pd* data are from Ref. [40].

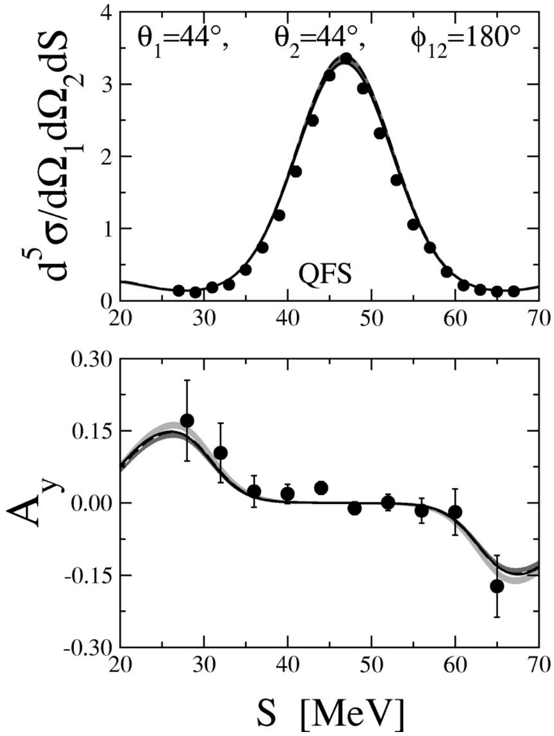


FIG. 17. $Nd$ breakup cross section in mb MeV$^{-1}$sr$^{-2}$ and nucleon analyzing power data at 65 MeV in comparison to theory. Quasifree scattering (QFS) configuration is shown. Bands and curves as in Fig. 1. The $pd$ data are from Ref. [40].

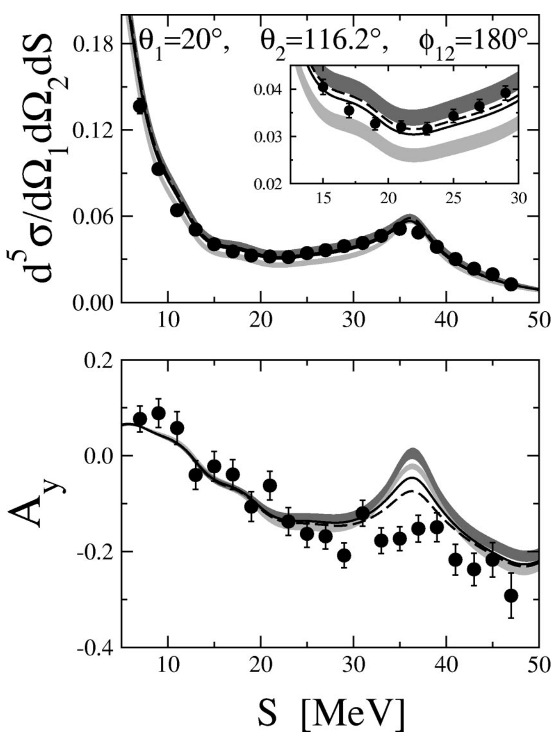


FIG. 18. $Nd$ breakup cross section in mb MeV$^{-1}$sr$^{-2}$ and nucleon analyzing power data at 65 MeV in comparison to theory. Collinear (COLL) configuration is shown. Bands and curves as in Fig. 1. The $pd$ data are from Ref. [39].

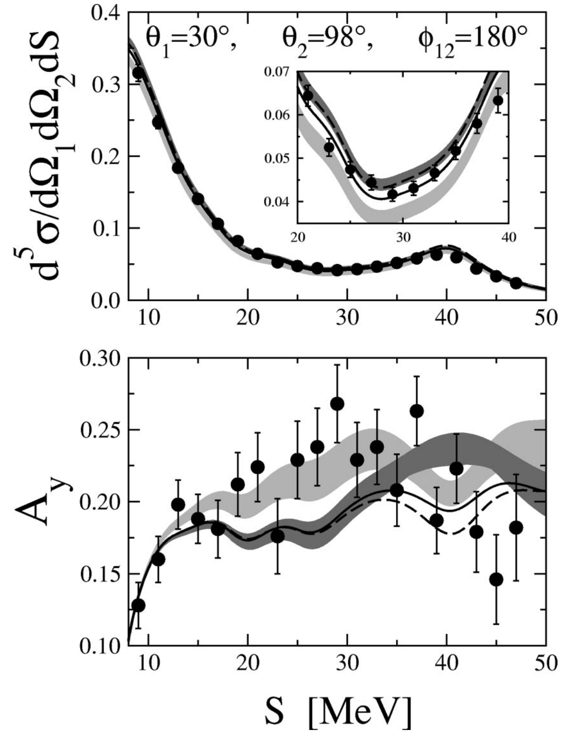


FIG. 19. $Nd$ breakup cross section in mb MeV$^{-1}$sr$^{-2}$ and nucleon analyzing power data at 65 MeV in comparison to theory. Collinear (COLL) configuration is shown. Bands and curves as in Fig. 1. The $pd$ data are from Ref. [39].

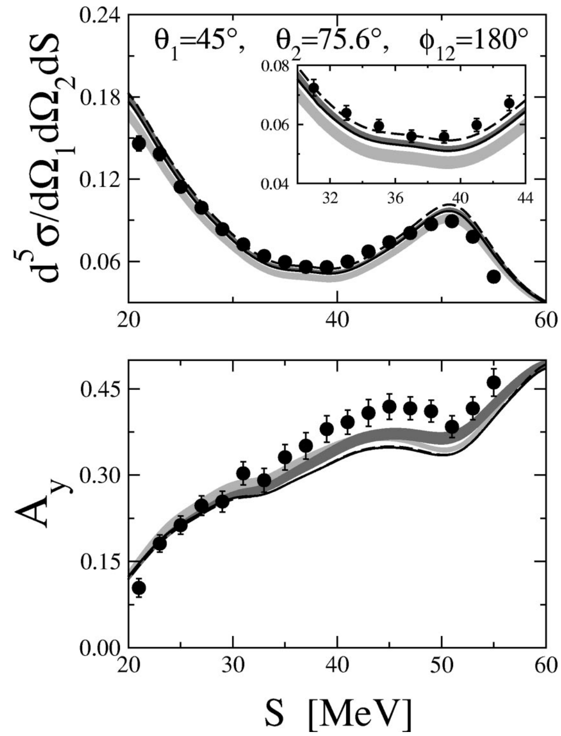


FIG. 20. $Nd$ breakup cross section in mb MeV$^{-1}$sr$^{-2}$ and nucleon analyzing power data at 65 MeV in comparison to theory. Collinear (COLL) configuration is shown. Bands and curves as in Fig. 1. The $pd$ data are from Ref. [39].

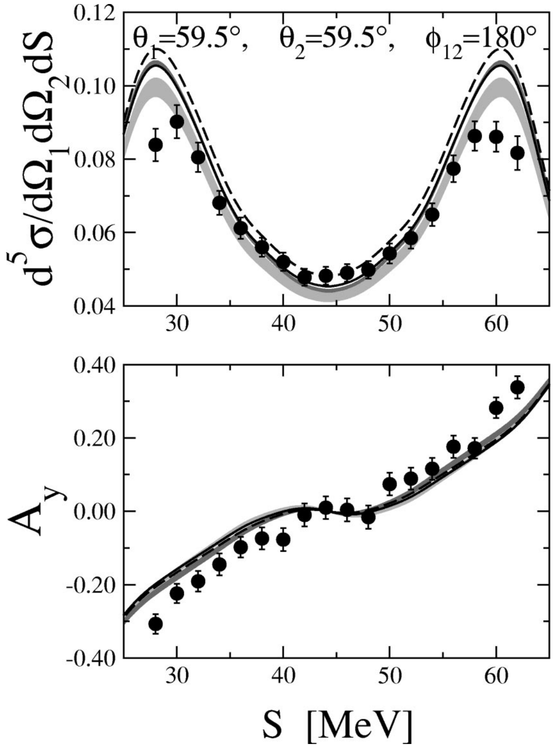


FIG. 21. *Nd* breakup cross section in mb MeV$^{-1}$sr$^{-2}$ and nucleon analyzing power data at 65 MeV in comparison to theory. Collinear (COLL) configuration is shown. Bands and curves as in Fig. 1. The *pd* data are from Ref. [39].

the error bars but 3NFs move theory away from the data. In the other case, a COLL one, neither *NN* forces alone nor the addition of 3NFs leads to an agreement with the data.

As at 13 MeV the SSS configuration poses a question. It has been measured at several energies. In all cases the *pd* data lie below the theoretical predictions, but this discrepancy decreases with increasing energy (about 15% at 10.5 MeV [19,20] and 13 MeV and about 7% at 19 MeV [29] and 65 MeV). Because of that decrease and the relative small 3NF effects one faces possibly again *pp* Coulomb force effects.

For $A_y$, as for $\sigma$, in the cases where the two bands are narrow and essentially overlapping there is agreement with the data with the exception of the configuration (59.5°, 59.5°, 180°) (see Fig. 21), where theory is partially below and partially above the data. When the bands are wider and clearly distinct unfortunately the data scatter a lot [see the configurations (30°, 59.5°, 180°): Fig. 16, (20°, 116.2°, 180°): Fig. 18, (30°, 98°, 180°): Fig. 19]. There are two more cases with less narrow bands [(45°, 75.6°, 180°): Fig. 20 and (20°, 75.6°, 180°): Fig. 24], where the data appear to differ from theory.

Further breakup data at and around 65 MeV can be found in Refs. [30,39–41,44–47]. Again we ask, whether the sensitive regions for 3NF effects according to paper I have been included in the existing data base. Unfortunately this is again not the case. The sensitive regions for the cross section and $A_y$ are around $\theta_1 \sim 20°, \theta_2 \sim 10°$ (and vice versa), and $0° \leqslant \phi_{12} \leqslant 60°$. Though the configuration (30°,98°,180°), for

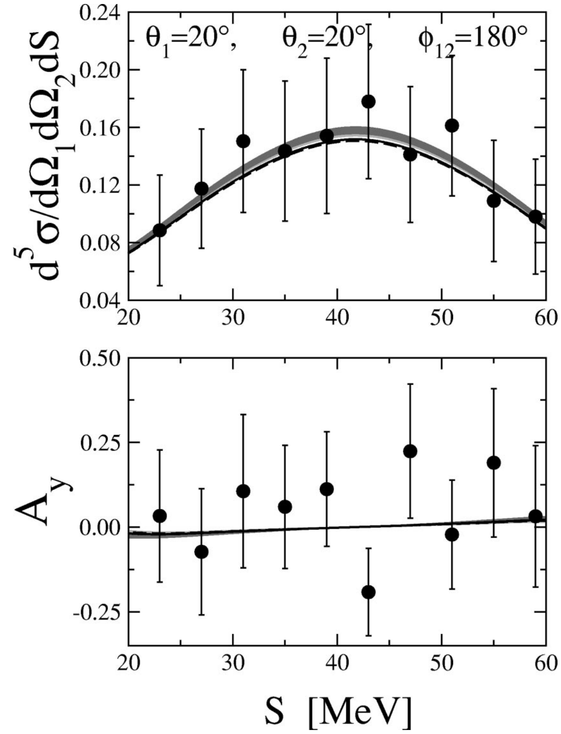


FIG. 22. *Nd* breakup cross section in mb MeV$^{-1}$sr$^{-2}$ and nucleon analyzing power data at 65 MeV in comparison to theory. Unspecific configuration is shown. Bands and curves as in Fig. 1. The *pd* data are from Ref. [41].

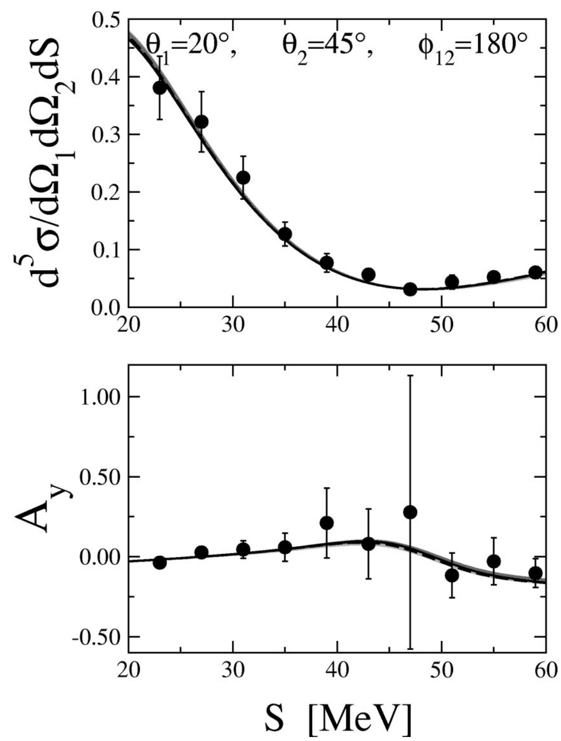


FIG. 23. *Nd* breakup cross section in mb MeV$^{-1}$sr$^{-2}$ and nucleon analyzing power data at 65 MeV in comparison to theory. Unspecific configuration is shown. Bands and curves as in Fig. 1. The *pd* data are from Ref. [41].

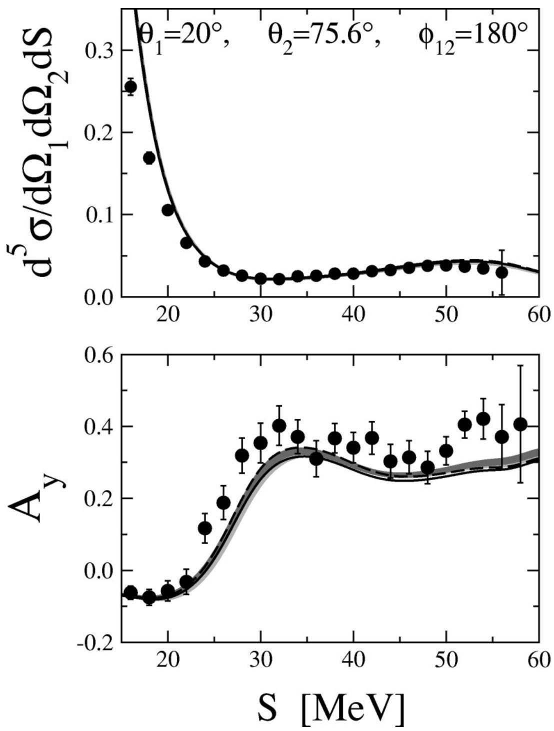


FIG. 24. Nd breakup cross section in mb MeV$^{-1}$sr$^{-2}$ and nucleon analyzing power data at 65 MeV in comparison to theory. Unspecific configuration is shown. Bands and curves as in Fig. 1. The *pd* data are from Ref. [41].

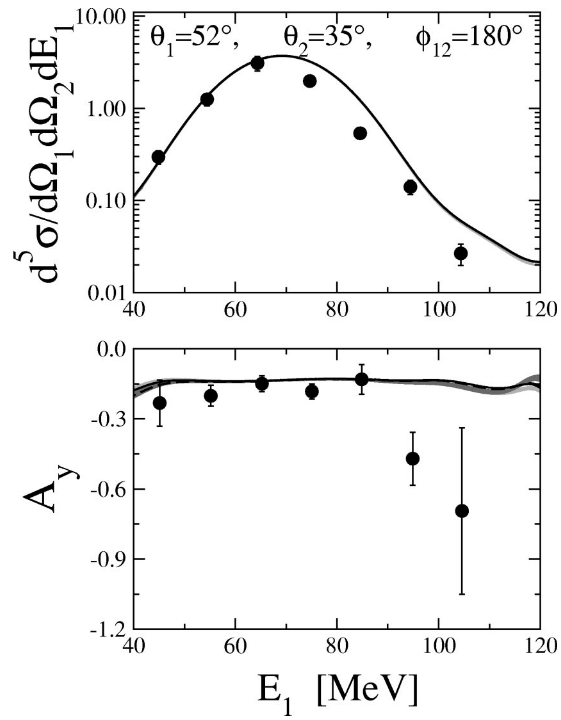


FIG. 26. *Nd* breakup cross section in mb MeV$^{-1}$sr$^{-2}$ and nucleon analyzing power data at 200 MeV in comparison to theory. Bands and curves as in Fig. 1. The *pd* data are from Ref. [17].

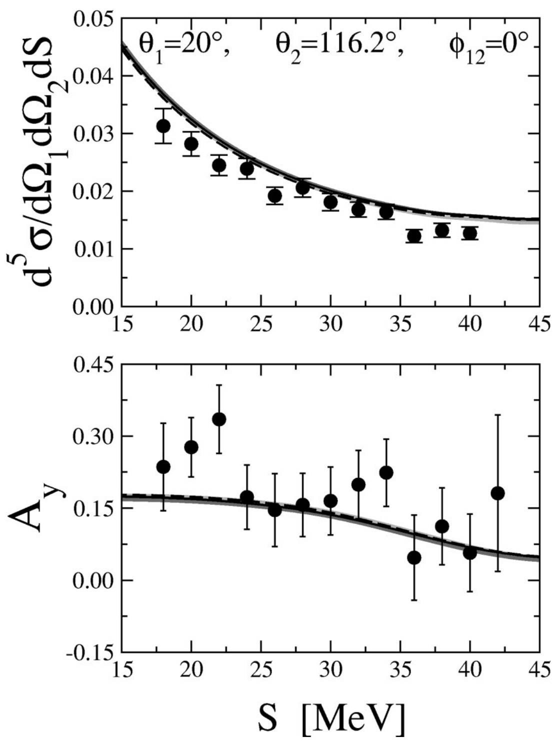


FIG. 25. *Nd* breakup cross section in mb MeV$^{-1}$sr$^{-2}$ and nucleon analyzing power data at 65 MeV in comparison to theory. Unspecific configuration is shown. Bands and curves as in Fig. 1. The *pd* data are from Ref. [41].

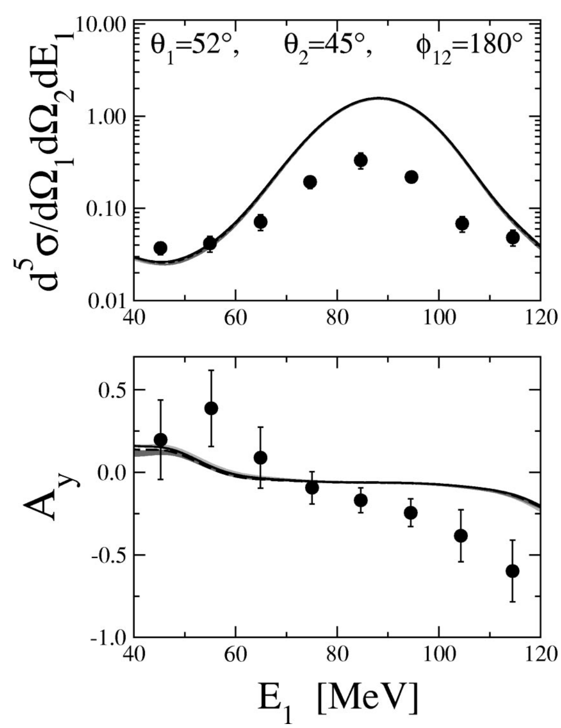


FIG. 27. *Nd* breakup cross section in mb MeV$^{-1}$sr$^{-2}$ and nucleon analyzing power data at 200 MeV in comparison to theory. Bands and curves as in Fig. 1. The *pd* data are from Ref. [17].

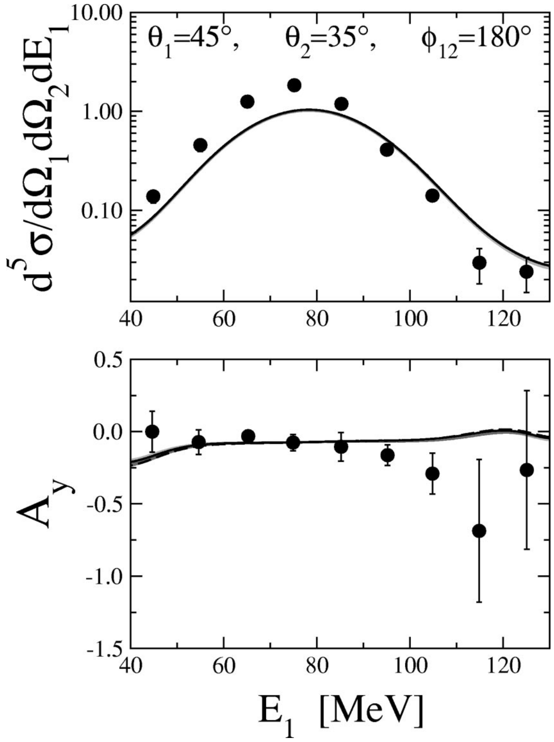


FIG. 28. $Nd$ breakup cross section in mb MeV$^{-1}$sr$^{-2}$ and nucleon analyzing power data at 200 MeV in comparison to theory. Bands and curves as in Fig. 1. The $pd$ data are from Ref. [17].

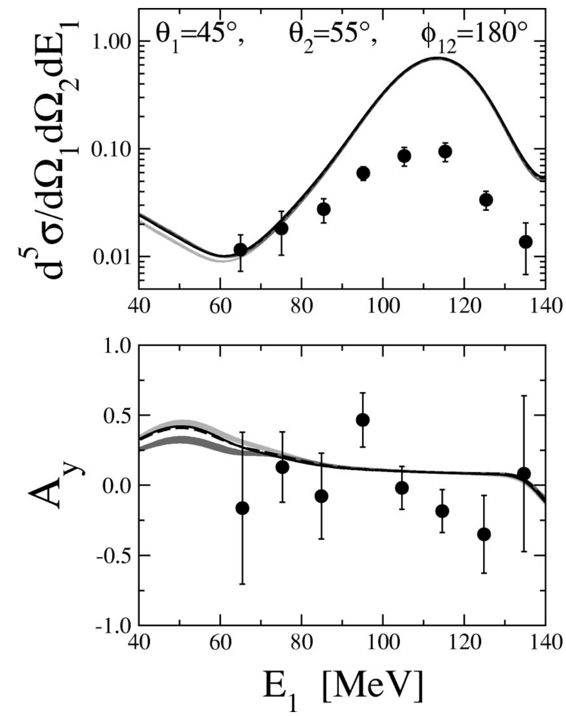


FIG. 30. $Nd$ breakup cross section in mb MeV$^{-1}$sr$^{-2}$ and nucleon analyzing power data at 200 MeV in comparison to theory. Bands and curves as in Fig. 1. The $pd$ data are from Ref. [17].

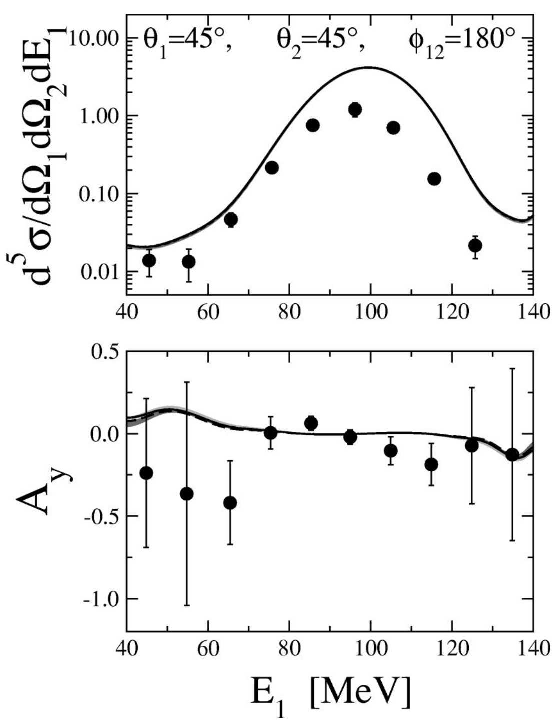


FIG. 29. $Nd$ breakup cross section in mb MeV$^{-1}$sr$^{-2}$ and nucleon analyzing power data at 200 MeV in comparison to theory. Bands and curves as in Fig. 1. The $pd$ data are from Ref. [17].

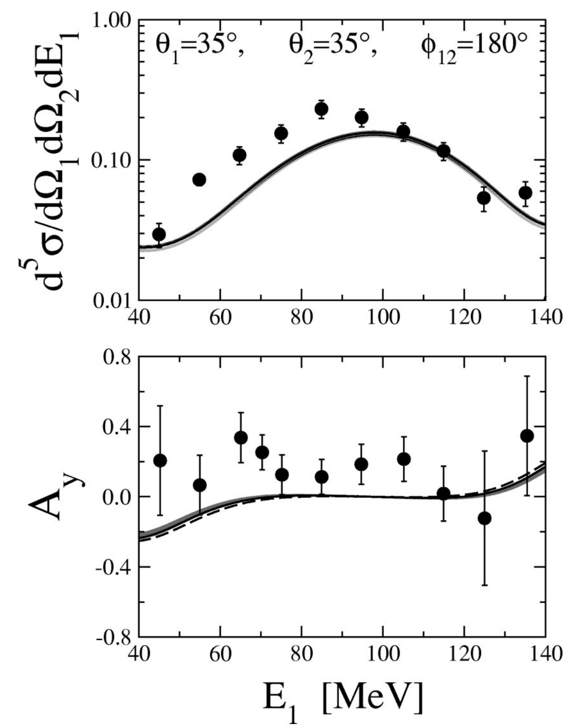


FIG. 31. $Nd$ breakup cross section in mb MeV$^{-1}$sr$^{-2}$ and nucleon analyzing power data at 200 MeV in comparison to theory. Bands and curves as in Fig. 1. The $pd$ data are from Ref. [17].

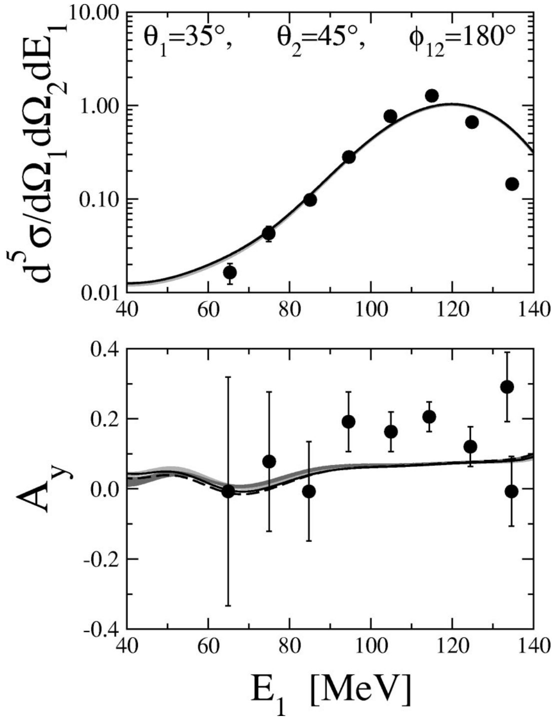


FIG. 32. *Nd* breakup cross section in mb MeV$^{-1}$sr$^{-2}$ and nucleon analyzing power data at 200 MeV in comparison to theory. Bands and curves as in Fig. 1. The *pd* data are from Ref. [17].

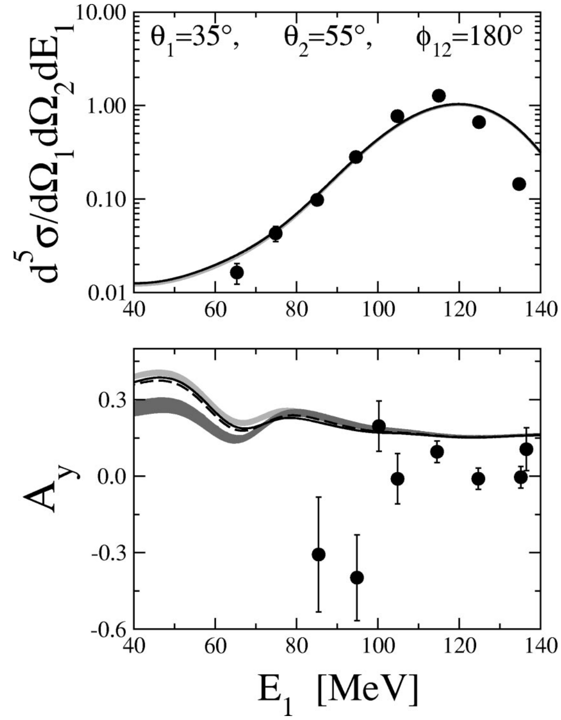


FIG. 33. *Nd* breakup cross section in mb MeV$^{-1}$sr$^{-2}$ and nucleon analyzing power data at 200 MeV in comparison to theory. Bands and curves as in Fig. 1. The *pd* data are from Ref. [17].

instance, in case of $A_y$ shows an interesting sensitivity to 3NFs, the effects are only of 30%, whereas effects of up to 100% and higher are predicted in the geometries just mentioned.

### C. Energy 200 MeV

In Figs. 26–33 we show a comparison of our theoretical predictions with the *pd* data of Ref. [17] for the cross section $d^5\sigma/d\Omega_1 d\Omega_2 dE_1$ and the nucleon analyzing power $A_y$. For the cross section the two bands are very narrow and overlapping. Thus we predict practically no 3NF effects. It is no surprise, since most of the configurations are in the vicinity of QFS. The comparison with the data, however, shows striking disagreements in most cases. Though the shapes are generally quite well reproduced, the magnitudes are wrong. This is alarming, since the current nuclear forces fail strongly. Note, however, we have no estimate for relativistic effects, which at this high energy can contribute both kinematically and dynamically.

Also in case of $A_y$ the two bands are mostly rather narrow and overlapping. Since some of the data have large error bars, agreement or disagreement of theory and data is not clear.

We are not aware of other breakup data in that energy region. The sensitive regions for 3NF effects are around $\theta_1 \sim 15° \sim \theta_2$ and $0° \leqslant \phi_{12} \leqslant 20°$ for the cross section and $\theta_1 \sim 100°$, $\theta_2 \sim 30°$ (and vice versa) and $\phi_{12} \sim 180°$ for $A_y$.

## III. SUMMARY

We compared modern *NN* force predictions alone and together with current 3NF models to a selected set of *Nd* breakup cross sections and analyzing power data at 13, 65, and 200 MeV. Though in most cases the agreement was good, we also found cases with striking discrepancies between theory and experiment. The discrepancies showed up in the SSS, QFS, and some unspecified geometries at low energies. Severe discrepancies are also present in the cross sections at 200 MeV. In all those cases the 3NF effects predicted by the current models are very small. At 200 MeV we cannot exclude that at least one reason for the discrepancy might lie in the totally neglected relativistic effects. At the lower energies *pp* Coulomb effects, not included in our theoretical description, might also play a role. In case of the analyzing power $A_y$ we found some discrepancies at 65 MeV, which point to deficiencies in the current nuclear force models. Some configurations with interesting theoretical 3NF effects at this energy could not be checked conclusively against experiment, since there is a big scatter in the available data.

The experiments performed so far show that it is rather difficult to find by chance a configuration with large 3NF effects. Therefore the breakup experiments should be guided by theoretical predictions such as the one in paper I. Also the present day *Nd* breakup data set is much poorer than the elastic scattering one, which calls for more data. Especially cross section and analyzing power measurements at higher energies in configurations where large 3NF effects have been predicted are highly desirable.

## ACKNOWLEDGMENTS

This work was supported by the Polish Committee for Scientific Research (Grant Nos. 2P03B02818 and 5P03B12320), the Deutsche Forschungsgemeinschaft (J.G.), and the NSF (Grant No. PHY0070858). One of us (W.G.) would like to thank the Foundation for Polish Science for the financial support during his stay in Cracow. R.S. thanks the Foundation for Polish Science for financial support. The numerical calculations have been performed on the Cray T90 and T3E of the NIC in Jülich, Germany.



[1] J. Kuroś-Żołnierczuk, H. Witała, J. Golak, H. Kamada, A. Nogga, R. Skibiński, and W. Glöckle, Phys. Rev. C **66**, 024003 (2002), preceding paper.
[2] R.B. Wiringa, V.G.J. Stoks, and R. Schiavilla, Phys. Rev. C **51**, 38 (1995).
[3] R. Machleidt, F. Sammarruca, and Y. Song, Phys. Rev. C **53**, R1483 (1996).
[4] V.G.J. Stoks, R.A.M. Klomp, C.P.F. Terheggen, and J.J. de Swart, Phys. Rev. C **49**, 2950 (1994).
[5] S.A. Coon *et al.*, Nucl. Phys. **A317**, 242 (1979).
[6] S.A. Coon and W. Glöckle, Phys. Rev. C **23**, 1790 (1981).
[7] A. Nogga, H. Kamada, and W. Glöckle, Phys. Rev. Lett. **85**, 944 (2000).
[8] B.S. Pudliner, V.R. Pandharipande, J. Carlson, S.C. Pieper, and R.B. Wiringa, Phys. Rev. C **56**, 1720 (1997).
[9] J.L. Friar, D. Hüber, and U. van Kolck, Phys. Rev. C **59**, 53 (1999).
[10] D. Hüber, J.L. Friar, A. Nogga, H. Witała, and U. van Kolck, Few-Body Syst. **30**, 95 (2001).
[11] W. Glöckle, H. Witała, D. Hüber, H. Kamada, and J. Golak, Phys. Rep. **274**, 107 (1996).
[12] G.J.F. Blommestijn, R. van Dantzig, Y. Haitsma, R.B.M. Mooy, and I. Slaus, Nucl. Phys. **A365**, 202 (1981).
[13] W.M. Kloet and J.A. Tjon, Nucl. Phys. **A210**, 380 (1973); Ann. Phys. (N.Y.) **79**, 407 (1973).
[14] St. Kistryn *et al.*, Nucl. Phys. **A689**, 345c (2001).
[15] K. Bodek (private communication).
[16] R. Bieber *et al.*, Nucl. Phys. **A684**, 536c (2001).
[17] W. Pairsuwan *et al.*, Phys. Rev. C **52**, 2552 (1995).
[18] J. Strate *et al.*, Nucl. Phys. **A501**, 51 (1989).
[19] M. Stephan *et al.*, Phys. Rev. C **39**, 2133 (1989).
[20] K. Gebhardt *et al.*, Nucl. Phys. **A561**, 232 (1993).
[21] C. Howell *et al.*, Nucl. Phys. **A631**, 692c (1998).
[22] H. Setze *et al.*, in *14th International Conference on Few Body Problems in Physics*, Williamsburg, VA, edited by Franz Gross, AIP Conf. Proc. No. 334 (AIP, Woodbury, 1995), p. 463.
[23] H. Setze *et al.*, Phys. Lett. B **388**, 229 (1996).
[24] W. Tornow *et al.*, Few-Body Syst., Suppl. **8**, 163 (1995).
[25] V. Huhn *et al.*, Phys. Rev. Lett. **85**, 1190 (2000).
[26] V. Huhn *et al.*, Phys. Rev. C **63**, 014003 (2001).
[27] F. Correll *et al.*, Nucl. Phys. **A475**, 407 (1987).
[28] G. Rauprich *et al.*, Nucl. Phys. **A535**, 313 (1991).
[29] H. Patberg *et al.*, Phys. Rev. C **53**, 1497 (1996).
[30] L. Qin *et al.*, Nucl. Phys. **A587**, 252 (1995).
[31] F. Foroughi *et al.*, Nucl. Phys. **A346**, 139 (1980).
[32] M. Karus *et al.*, Phys. Rev. C **31**, 1112 (1985).
[33] M. Przyborowski *et al.*, Phys. Rev. C **60**, 064004 (1999).
[34] H. Paetz gen. Schieck *et al.*, Few-Body Syst. **30**, 81 (2001).
[35] R. Grossmann *et al.*, Nucl. Phys. **A603**, 161 (1996).
[36] M. Zadro *et al.*, Nuovo Cimento A **107**, 185 (1994).
[37] D.E. González Trotter *et al.*, Phys. Rev. Lett. **83**, 3788 (1999).
[38] W. von Witsch (private communication).
[39] M. Allet *et al.*, Phys. Rev. C **50**, 602 (1994).
[40] J. Zejma *et al.*, Phys. Rev. C **55**, 42 (1997).
[41] K. Bodek *et al.*, Few-Body Syst. **30**, 65 (2001).
[42] H. Witała, W. Glöckle, and Th. Cornelius, Few-Body Syst. **6**, 79 (1989).
[43] E. Alt and M. Rauh, Few-Body Syst. **17**, 121 (1994).
[44] M. Allet *et al.*, Few-Body Syst., Suppl. **7**, 243 (1994).
[45] M. Allet *et al.*, Few-Body Syst. **20**, 27 (1996).
[46] M. Allet *et al.*, Few-Body Syst., Suppl. **8**, 49 (1996).
[47] D.A. Low *et al.*, Phys. Rev. C **44**, 2276 (1991).